Synthetic Peptides Corresponding to the Four P Regions of *Electrophorus electricus* Na^+ Channel: Interaction with and Organization in Model Phospholipid Membranes†

Yehonathan Pouny and Yechiel Shai*

Department of Membrane Research and Biophysics, Weizmann Institute of Science, Rehovot, 76100 Israel

Received January 19, 1995; Revised Manuscript Received March 2, 1995®

ABSTRACT: The hydropathy plot of the α subunit of the voltage-gated Na^+ channel reveals four homologous repeats, each of which is homologous to *Shaker* type K^+ channel monomer and contains six putative transmembrane segments and a hydrophobic segment within the loop connecting transmembrane segments S5 and S6. Current models predict that the four homologous segments [designated H5 or P regions (PR)] from the S5-S6 loop of each repeat lie in the aqueous pore. Peptides corresponding to the P regions of the four domains of the *Electrophorus electricus* (eel) Na^+ channel (25−36 aa long, designated as PR-I, PR-II, PR-III, and PR-IV) and a 23-mer preceding PR-II (designated pre-PR-II) were synthesized and flourescently labeled. The segments were then structurally and functionally characterized for their interaction with phospholipid membranes. Although the sequences of the four P regions are significantly different, they all bind to zwitterionic phospholipid membranes with similar partition coefficients (~10^4 M^{-1}). The pre-PR-II does not bind membranes at all. Resonance energy transfer measurements, between donor/acceptor-labeled pairs of peptides, revealed that besides the PR-I/PR-III pair, all other pairs form heteroaggregates but do not coassemble with unrelated membrane-bound peptide. Circular dichroism (CD) spectroscopy revealed that PR-I, PR-II, and PR-III adopt similar partial α-helical structures (~30%) in 40% trifluoroethanol and in solutions of 1% sodium dodecylsulfate (SDS). The PR-IV (36 aa) adopts ~18% α-helical structure, and pre-PR-II gives a low CD signal. These findings are in line with proposed models in which the P regions are packed in close proximity in the lumen of the hydrophobic core of the channel. Furthermore, the finding that the PRs adopt similar partial α-helical structures in two different hydrophobic environments might suggest that partial α-helical structures also exist in the native channel as proposed by recent models. The results are discussed in terms of proposals that various regions of membrane proteins participate in driving folding or oligomerization of the parent molecules.

The voltage-gated Na^+ channels are integral membrane proteins that are responsible for the initial inward current during the depolarization phase of an action potential [see reviews by Armstrong (1992) and Catterall (1992)]. The functional channel consists of a large α subunit of molecular mass of 230−270 kDa that in some tissues is associated with small β subunits. The hydropathy plot suggests that the α subunit is composed of four homologous repeats, each of which contains six putative transmembrane segments and a hydrophobic segment within the loop connecting transmembrane segments S5 and S6 (Guy & Seetharamulu, 1986). Each repeat is also homologous to the *Shaker* type K^+ channel subunit. Essentially all models for the structure of the voltage-gated ion channels include a transmembrane pore in the center of a square array of the homologous transmembrane domains (Greenblatt et al., 1985; Noda et al., 1986a,b, 1988; Durell & Guy, 1992; Sato & Matsumoto., 1992). Each domain would contribute one-fourth of the wall of the pore. Identification of the segments of these proteins that line the transmembrane pore and define the properties of the channels, as well as those segments that contribute to the correct assembly of the channel, is of great interest and importance.

Due to the paucity of X-ray diffraction data, the structures of ion channels are modeled on the basis of hydropathy plots, analytical methods that predict local secondary structures for short segments, energy minimization, and functional studies combined with site-directed mutagenesis. Several of these studies conducted with K^+ channels indicated that regions within the loops (termed H5) connecting S5 and S6 of four monomers line the lumen of the channel and control its selectivity and its sensitivity to channel blockers (MacKinnon & Yellen, 1990; Heginbotham & MacKinnon, 1992; MacKinnon et al., 1990; MacKinnon & Miller, 1989; Yellen et al., 1991; Hartmann et al.,1991; Yool & Schwarz, 1991). Due to the homology between the *Shaker* type K^+ channel and one repeat of the Na^+ channel, the H5 (or P) regions of both types of channels are assumed to have similar function. Indeed, studies performed with sodium channels (Heinemann et al., 1992; Backx et al., 1992), calcium channels (Tang et al., 1993), and cyclic nucleotide-gated channels (Goulding et al., 1993) indicated that the P regions are intimately involved in channel selectivity. Furthermore, point mutations

† This research was supported in part by the Basic Research Foundation, administered by the Israel Academy of Sciences and Humanities, and by the Joseph Cohn Center for Biomembrane Research at the Weizmann Institute of Science. Y.S. is an Incumbent of the Adolpho and Evelyn Blum Career Development Chair in Cancer Research.

* To whom correspondence should be addressed at the Department of Membrane Research and Biophysics, Weizmann Institute of Science, Rehovot, 76100, Israel. Tel: 972-8-342711. Fax: 972-8-344112. E-mail: BMSHAI@WIEZMANN.WEIZMANN.AC.IL.

® Abstract published in *Advance ACS Abstracts,* June 1, 1995.

0006-2960/95/0434-7712$09.00/0

in the P regions of Na^+ channels have caused significant changes in both pore permeability (Pusch et al., 1991) and affinity to channel blockers (Terlau et al., 1991; Kontis & Goldin, 1993). However, while four identical H5 segments are assumed to line the pore of K^+ channels, the four P regions of the Na^+ channel are not identical, though they share significant homology. Furthermore, the P region of the *Shaker* type K^+ channel appears to contain ~21 amino acids out of the 40 that build the loop connecting helices 5 and 6. In the Na^+ channel, the homologous loops are composed of 70−110 amino acids, from which only ~21 amino acids are predicted to possess the properties of the H5 region of the K^+ channel. Recently we have shown that synthetic peptides resembling the P region of the *Shaker* K^+ channel adopt a low level of α-helicity in hydrophobic environments, bind phospholipid membranes, and self-assemble in their membrane-bound state, but do not co-assemble with unrelated membrane-bound peptides (Peled & Shai, 1993). These results support the notion that they are packed in close proximity in the native channel and that they have a possible role in assisting in the correct assembly of the channel.

In this study a spectrofluorometric approach was utilized to investigate the properties of the four P regions of the *Electrophorus electricus* (eel) Na^+ channel. Peptides resembling the consensus sequences of the P regions (PR)[1] of domains I, II, and III and the N-terminal extended form of repeat VI (aa 345−370, aa 734−759, aa 1197−1221, and aa 1477−1512, respectively) of the *Electrophorus electricus* (eel) Na^+ channel were synthesized, fluorescently labeled, and structurally and functionally characterized for their interaction with phospholipid membranes. A 23-mer resembling the sequence preceding PR-II (pre-PR-II, aa 711−733) was also synthesized and, along with pardaxin, a channel-forming polypeptide, served as a control peptide in these studies. We found that the PRs, but not pre-PR-II, strongly bind phospholipid membranes with similar partition coefficients, which are comparable to what has been found for the PR of the *Shaker* K^+ channel. Furthermore, the PRs adopt partial α-helical structures in two hydrophobic environments as determined by CD spectroscopy, and they form heteroaggregates but do not bind unrelated membrane-bound pardaxin. The results are discussed in terms of their relevance to the proposed model for the structure of Na^+ channels and to general aspects of molecular recognition between membrane-bound polypeptides.

MATERIALS AND METHODS

Materials. BOC amino acid−PAM [(phenylacetamido)-methyl] resins were purchased from Applied Biosystems (Foster City, CA), and BOC amino acids were obtained from Peninsula Laboratories (Belmont, CA). Other reagents for peptide synthesis included trifluoroacetic acid (TFA) (Sigma), *N,N*-diisopropylethylamine (DIEA) (Aldrich, distilled over ninhydrin), dicyclohexylcarbodiimide (DCC) (Fluka), 1-hydroxybenzotriazole (HOBT) (Pierce), methylene chloride, and dimethyl formamide (DMF) (Bio-Lab). Egg phosphatidylcholine (PC) was purchased from Lipid Products (South Nutfield, U.K). Cholesterol (extra pure) was supplied by Merck (Darmstadt, Germany) and recrystallized twice from ethanol. 5-(and-6)-Carboxytetramethylrhodamine succinimidyl ester was obtained from Molecular Probes (Eugene, OR). 4-Fluoro-7-nitrobenz-2-oxa-1,3-diazole (NBD-F) was obtained from Sigma. All other reagents were of analytical grade. Buffers were prepared using double glass distilled water.

Peptide Synthesis and Fluorescence Labeling. The peptides were synthesized by the solid-phase method on amino acid−PAM resins (0.7 mequiv) (Merrifield et al., 1982). At the end of the synthesis, the resin-bound peptides were treated for 3 min with 20% piperidine in dimethyl formamide to remove the formyl protecting group from the tryptophan, cleaved from the resins by HF, and finally extracted with ether after HF evaporation. The synthesized peptides were purified by RP-HPLC on a C_4 reversed-phase Vydac column (300-Å pore size). The column was eluted in 40 min, at a flow rate of 0.6 mL/min, using a linear gradient of 25−80% acetonitrile in water in the presence of 0.1% TFA (v/v). The purified peptides were shown to be homogeneous (~99%) by analytical HPLC. The peptides were subjected to amino acid analysis to confirm their composition.

The N-termini of the resin-bound peptides were fluorescently labeled as previously described (Rapaport & Shai, 1991, 1992). Resin-bound peptides (30 mg, ~10 μmol) were treated with TFA (50%, v/v, in methylene chloride) to remove the BOC protecting group from the N-terminal amino group of the attached peptides. The resin-bound peptides were then reacted with either (i) 5-(and-6)-carboxytetramethylrhodamine succinimidyl ester (5−7 equiv) in dry dimethyl formamide containing 2.5%, v/v, diisopropylethylamine or (ii) NBD-F in dry dimethyl formamide. These two separate reactions led to the formation of resin-bound N^1-Rho-peptides or N^1-NBD-peptides, respectively. After 72 h, the mixtures were washed thoroughly with methylene chloride. The peptides were then cleaved from the resins by HF and purified by reversed-phase HPLC as described above.

Preparation of Small and Large Unilamellar Vesicles. Small unilamellar vesicles (SUV) were prepared by sonication of egg PC as previously described (Rapaport & Shai, 1991). Briefly, dry lipid and cholesterol (10:1, w/w) were dissolved in a $CHCl_3$/MeOH mixture (2:1, v/v). The solvents were then evaporated under a stream of nitrogen, and the lipids (at a concentration of 7.2 mg/mL) were put under vacuum for 1 h. and then resuspended in the appropriate buffer, via vortex mixing. The resultant lipid dispersion was then sonicated for 10−30 min in a bath type sonicator (Model G1125SP1, Laboratory Supplies Company Inc., New York) until clear. The lipid concentration was determined by phosphorus analysis (Bartlett et al., 1959). Vesicles were visualized using a JEOL JEM 100B electron microscope (Japan Electron Optics Laboratory Co., Tokyo). Vesicles prepared in this fashion are unilamellar, with an average diameter of 20−50 nm (Papahadjopoulos & Miller, 1967).

LUV were prepared from phospholipids as follows. Dry lipids were hydrated in buffer and dispersed by vortexing to produce large multilamellar vesicles. The lipid suspension was freeze-thawed five times and then extruded through polycarbonate membrane filters (Poretics Corp., Livermore, CA) in an extruder (Lipex Biomembranes Inc., Vancouver,

[1] Abbreviations: BOC, butyloxycarbonyl; CD, circular dichroism; LUV, large unilamellar vesicles; NBD, 7-nitrobenz-2-oxa-1,3-diazol-4-yl; Pam, (phenylacetamido)methyl; PC, egg phosphatidylcholine; PR, pore region; Rho, tetramethylrhodamine; SUV, small unilamellar vesicles.

Table 1: Sequences and Designations of the Peptides Investigated

no.	designation	modification	sequence
1	PR-I	X = H	X-HN-^{345}DNFAWTFLCLFRLMLQDYWENLYQMT^{370}-COOH
2	NBD-PR-I	X = NBD	
3	Rho-PR-I	X = Rho	
4	PR-II	X = H	X-HN-^{734}DFFHSFLIVFRALCGEWIETMWDCME^{759}-COOH
5	NBD-PR-II	X = NBD	
6	Rho-PR-II	X = Rho	
7	PR-III	X = H	X-HN-^{1197}DNAGMGYLSLLQVSTFKGWMDIMYA^{1221}-COOH
8	NBD-PR-III	X = NBD	
9	Rho-PR-III	X = Rho	
10	PR-IV	X = H	X-HN-^{1477}KKQGGVDDIFNFETFGNSMICLFEITTSAGWDGLLL^{1512}-COOH
11	NBD-PR-IV	X = NBD	
12	pre-PR-II	X = H	X-HN-^{711}GKNYKEYVCKISDDCELPRWHMN^{733}-COOH
13	NBD-pre-PR-II	X = NBD	
14	Rho-pardaxin	X = Rho	X-HN-GFFALIPKIISSPLFKTLLSAVGSALSSSGGQE-COOH

BC), twice with a pore diameter of 0.4 μm and then eight times with a pore diameter of 0.1 μm (Mayer et al., 1986). The size distribution of the vesicles was determined by dynamic light scattering in a Malvern 4700 submicron particle analyzer. The mean diameter was found to be 113 nm.

CD Spectroscopy. CD spectra were measured at room temperature using a Jasco J-500A spectropolarimeter after the instrument was calibrated with (+)-10-camphorsulfonic acid. A cylindrical fused quartz optical cell of 0.5 mm path length was used. Spectra were obtained at wavelengths of 250−190 nm. Eight scans were taken at a scan rate of 20 nm/min. The peptides were scanned at concentrations of 0.5−20 μM, in (A) 1% sodium dodecyl sulfate (SDS) in buffer containing 16.7 mM NaCl and 4.3 mM HEPES, pH 7, and (B) a mixture of 40% (v/v) TFE in H_2O. Fractional helicities (Greenfield & Fasman, 1969; Wu et al., 1981) were calculated as follows:

$$f_h = \frac{([\theta]_{222} - [\theta]^0_{222})}{[\theta]^{100}_{222}}$$

where $[\theta]_{222}$ is the experimentally observed mean residue ellipticity at 222 nm, and values for $[\theta]^0_{222}$ and $[\theta]^{100}_{222}$, corresponding to 0% and 100% (e.g., $[\theta]_{max} - [\theta]^0_{222}$) helix content at 222 nm, are estimated at −2000 and −30000 deg cm^2/dmol, respectively [modified from Chen et al. (1974) and Wu et al. (1981)].

NBD Fluorescence Measurements. Changes in the fluorescence of NBD-labeled peptides upon binding to vesicles were measured. NBD-labeled peptide (final concentration, 0.1 μM) was added to 100 μL of buffer (50 mM Na_2SO_4, 25 mM HEPES-SO_4^{-2}, pH 6.8) containing 600−1400 μM SUV composed of PC to establish a lipid/peptide ratio in which most of the peptide was bound to the lipids (lipid/peptide molar ratio, 6000:1−14000:1). After a 2-min incubation, emission spectra were recorded with a Perkin-Elmer LS-50B spectrofluorometer, with the excitation set at 470 nm, using a 10-nm slit, and the emission set at 530 nm, using a 5-nm slit.

Binding Experiments. The environmentally sensitive NBD fluorophore has been previously utilized for polarity and binding studies (Kenner & Aboderin, 1971; Frey & Tamm, 1990; Rapaport & Shai, 1991; Pouny et al., 1992). The binding experiments were conducted in two different ways depending on the peptide investigated. Briefly, either PC SUV were added successively to 0.1 μM of the more soluble NBD-labeled PR-I, PR-II, or PR-III or, alternatively, 0.04 μM of NBD-PR-IV was added to increasing concentrations of PC SUV in separate Eppendorf tubes. Fluorescence intensities were measured as a function of the lipid/peptide molar ratio on a Perkin-Elmer LS-50B spectrofluorometer, with the excitation set at 470 nm, using a 10-nm slit, and the emission set at 530 nm, using a 5-nm slit, in 3−5 separate experiments. To determine the extent of the lipids' contribution to any given signal, the readings observed when unlabeled peptides were titrated with lipid vesicles were subtracted as background from the recorded fluorescence intensities. The binding isotherms were analyzed as partition equilibria (Schwarz et al., 1986, 1987; Rizzo et al., 1987; Beschiaschvili & Seelig, 1990; Rapaport & Shai, 1991), using the following formula:

$$X_b^* = K_p^* C_f$$

where X_b^* is defined as the molar ratio of bound peptide per 60% of the total lipid, assuming that the peptides were initially partitioned only over the outer leaflet of the SUV, as has been previously suggested (Beschiaschvili & Seelig, 1990); K_p^* corresponds to the partition coefficient; and C_f represents the equilibrium concentration of free peptide in the solution. To calculate X_b, F_∞ (the fluorescence signal obtained when all of the peptide is bound to lipid) was extrapolated from a double-reciprocal plot of F (total peptide fluorescence) versus C_L (total concentration of lipids) (Schwarz et al., 1986). Knowing the fluorescence intensities of unbound peptide, F_0, and bound peptide, F, the fraction of membrane-bound peptide, f_b, could be calculated using the formula

$$f_b = (F - F_0)/(F_\infty - F_0)$$

The value of f_b having been calculated, it is then possible to calculate C_f, as well as the extent of peptide binding, X_b^*. The curves that result from plotting X_b^* versus free peptides, C_f, are referred to as the conventional binding isotherms.

Mutual Interactions as Determined by Resonance Energy Transfer (RET) Experiments. RET experiments were conducted as previously described (Gazit & Shai, 1993) using PC LUV. Fluorescence spectra were obtained at room temperature in a Perkin-Elmer LS-50B spectrofluorometer, with the excitation monochromator set at 450 nm with a 5-nm slit width. A lower wavelength was used to prevent partial excitation of rhodamine. Measurements were performed in a 3-mm path length quartz cuvette in a final reaction volume of 400 μL.

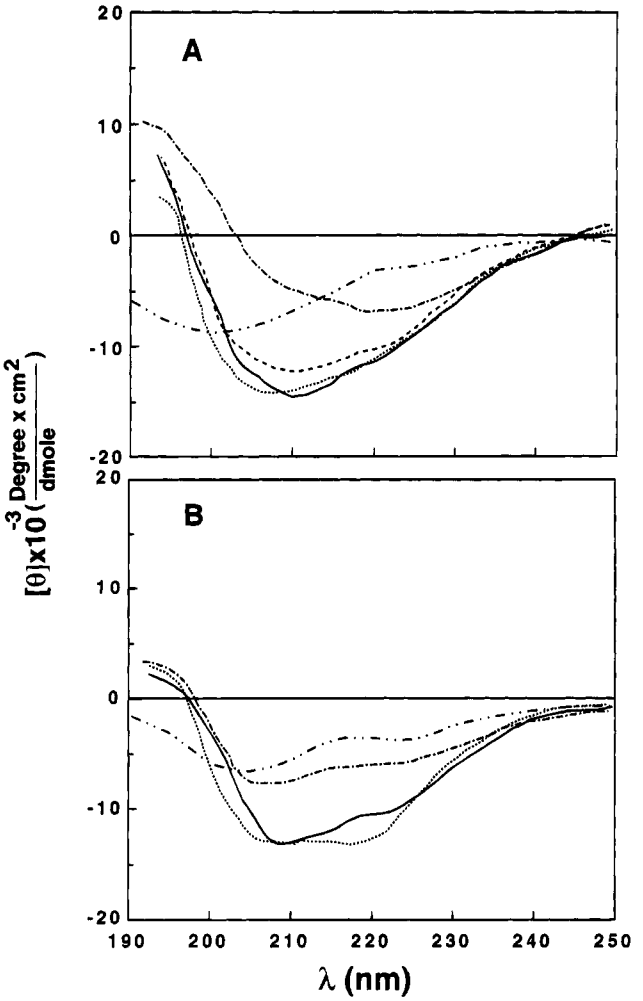

FIGURE 1: CD spectra of PR segments in (A) 40% TFA in water and (B) 1% SDS in buffer containing 16.7 mM NaCl and 4.3 mM HEPES, pH 7. Spectra were taken as described in Materials and Methods at peptide concentrations of 0.5×10^{-5} to 2.0×10^{-5} M: PR-I (—), PR-II (•••), PR-III (- - -), PR-IV (• — •), pre-PR-II (•• — ••).

The efficiency of energy transfer (E) was determined by the decrease in the quantum yield of the donor (NBD-labeled peptides) as a result of the addition of acceptor (Rho-labeled peptides). E was determined experimentally from the ratio of the fluorescence intensities of the donor in the presence (I_{da}) and in the absence (I_d) of the acceptor at the emission wavelength of the donor, after correcting for membrane light scattering and the contribution of the emission of the acceptor. The percentage value of E is given by the equation

$$E = (1 - I_{da}/I_d) \times 100$$

The correction for light scattering was made by subtracting the signal obtained when unlabeled analogues, at concentrations equal to the sum of the donor and the acceptor, were added to vesicles. The correction for the contribution of acceptor emission was made by subtracting the signal produced by the acceptor-labeled analogue in the presence of unlabeled donor peptide.

Mutual Interactions as Determined by NBD Fluorescence. NBD-labeled peptide (final concentration, 0.04 μM) was mixed with PC LUV (final concentration, 175 μM) in buffer (50 mM Na_2SO_4 and 25 mM HEPES-SO_4^{-2}, pH 6.8). Measurements were performed in a 3-mm path length quartz cuvette in a final reaction volume of 400 μL. Emission spectra were recorded at room temperature in a Perkin-Elmer LS-50B spectrofluorometer, with the excitation monochromator set at 470 nm.

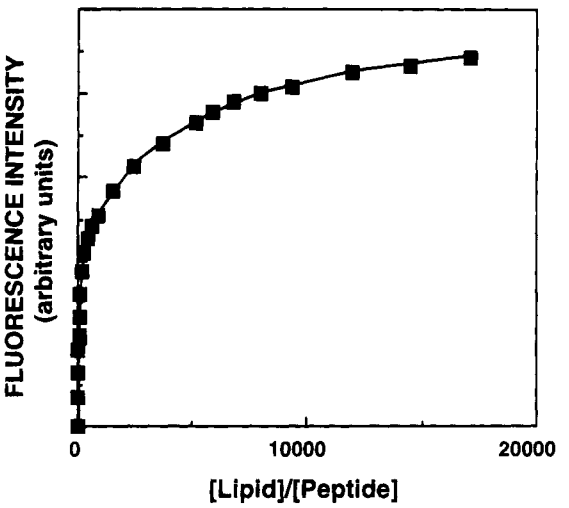

FIGURE 2: Increases in the fluorescence of NBD-PR-I upon titration with PC SUV. Peptide (0.1 μM total concentration) was titrated with PC vesicles with the excitation monitored at 470 nm and the emission recorded at 530 nm. The experiment was performed at room temperature in 50 mM Na_2SO_4 and 25 mM HEPES-SO_4^{-2}, pH 6.8.

The effect of the interaction between unlabeled peptide and a particular NBD-labeled peptide was determined as the percentage of the increase or decrease of the fluorescence intensity of the NBD upon the addition of the unlabeled peptide (0.04 μM). The correction for light scattering was made by subtracting the signal obtained when unlabeled analogues, at concentrations equal to the sum of the labeled and unlabeled peptides, were added to vesicles.

RESULTS

Synthesis and Fluorescence Labeling of the Peptides. Peptides with sequences identical to those of the four P regions of the *Electrophorus electricus* Na^+ channel were synthesized. Fluorescently labeled analogues were prepared by selectively attaching to the N-terminal amino acid of the peptides the fluorophores NBD (to serve in the binding experiments and as an energy donor) or Rho (to serve as an energy acceptor) (Rapaport & Shai, 1991, 1992; Pouny et al., 1992). PR-IV (aa 1484−1512) was very hydrophobic and therefore highly adsorbed onto the reversed-phase columns that were used. For this reason, a longer version was prepared (aa 1477−1512), which carries a few more polar residues. A 23-mer resembling the sequence preceding PR-II (aa 711−733) was also synthesized and, along with pardaxin, a channel-forming polypeptide, served as a control in these studies. Table 1 shows the sequences of the peptides and their designations.

Secondary Structure of H5 Segments. The secondary structures of the PR segments were estimated from their CD spectra in two hydrophobic environments: (i) in a mixture of 40% TFE in H_2O (Figure 1A) and (ii) in a membrane-mimetic environment of sodium dodecyl sulfate (1% SDS) micelles in buffer containing 16.7 mM NaCl and 4.3 mM HEPES, pH 7 (Figure 1B). Due to the low solubility of PR-III in the SDS buffer, its CD spectrum was obtained only in a TFE/H_2O mixture. The concentrations of the peptides were

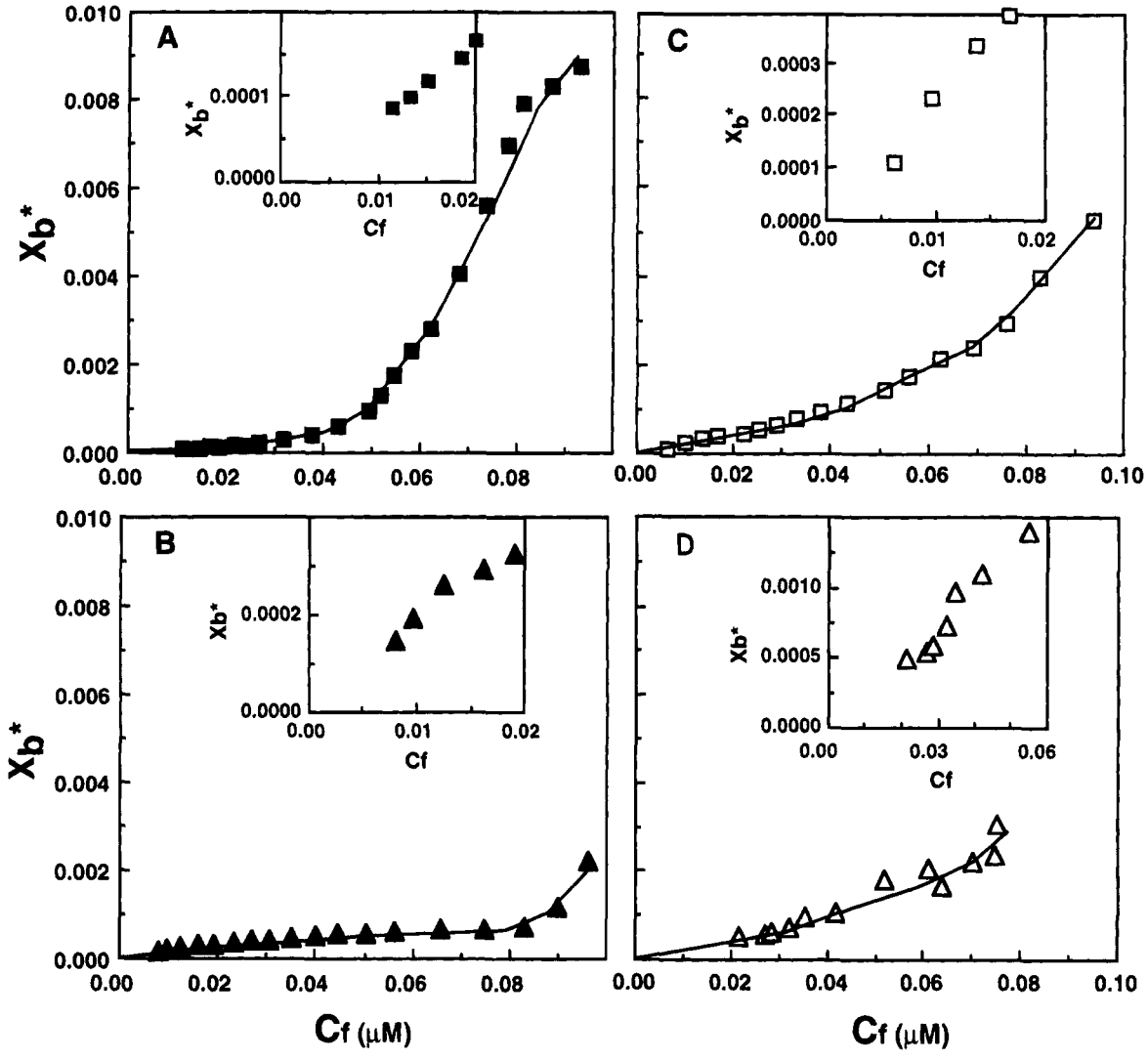

FIGURE 3: Binding isotherms of the PRs derived from the corresponding binding curves similar to that presented in Figure 2. The binding isotherms were derived by plotting X^*_b (molar ratio of bound peptide per 60% lipid) versus C_f (equilibrium concentration of free peptide in the solution). The insets show the low-concentration range of the main figures. Panels A, B, C, and D are for PR-I, PR-II, PR-III, and PR-IV, respectively.

Table 2: Mean Residual Ellipticities, $[\theta]_{222}$, and Percent of α-Helical Content of the Peptides Investigated Measured in 40% TFA/Water and in 1% SDS

peptide designation	$[\theta]_{222}$ [(degree cm^2)/dmol) 40% TFA/H_2O	$[\theta]_{222}$ [(degree cm^2)/dmol) 1% SDS	% of α-helix 40% TFA/H_2O	% of α-helix 1% SDS
PR-I	−10500	−10500	31	31
PR-II	−10500	−11900	31	33
PR-III	−10450	not determined	31	
PR-IV	−6950	−5900	18	14
pre-PR-II	−2500	−3200	2	4

5−20 μM as determined by amino acid analysis and UV absorption at 280 nm. The CD spectra of the peptides were not determined in the presence of phospholipid membranes for the following reason. We found in several other cases (Gazit & Shai, 1993; Shai et al., 1990) that CD spectra can be obtained at the optimal peptide/lipid molar ratio of 0.04, to avoid interference of light scattering due to high concentration of vesicles. Under these conditions the amounts of the peptides bound to the vesicles, as calculated from their binding isotherms (Figure 3), are 4−10%. Therefore, no significant signal should be obtained, as has been shown with helix-1 of the Bti toxin (Gazit & Shai, 1993).

The mean residual ellipticities $[\theta]_{222}$ and the corresponding α-helical contents (Wu et al., 1981) of the four PR peptides in 40% TFE and in 1% SDS in buffer are given in Table 2. The data reveal that although the PR segments from the different domains differ significantly in their primary sequences, they adopt similar partial α-helical structures (~30%). The lesser amount of α-helical structure observed in PR-IV is probably the result of the longer size of this peptide (i.e., ~18% helicity within a 36-mer corresponds to the same number of amino acids in an α-helical structure as ~31% helicity within a 25-mer). The CD signal of pre-PR-II at 222 nm was very low.

Localization of the NBD Moiety. The fluorescence emission spectra of NBD-labeled peptides were monitored in aqueous solutions at pH 6.8, with and without SUV composed of PC. Table 3 shows the emission maxima of all the PRs, including pre-PR-II, in buffer and in the presence of the vesicles. SUV were used to minimize light-scattering effects (Mao & Wallace, 1984), and the lipid/peptide molar ratio was elevated (6000:1−14000:1) so that the spectral contributions of free peptide would be negligible. When placed in buffer, the peptides exhibited emission maxima

Table 3: Emission Maxima, Calculated Partition Coefficients, and Enthalpies of Binding [Calculated According to Reynold et al. (1974)] of the Peptides Investigated

peptide designation	λ max (nm) buffer	λ max (nm) PC vesicles	K^*_p (M^{-1}) PC vesicles	$-\Delta G_{binding}$ (kcal/mol) PC vesicles
NBD-PR-I	546 ± 1	520 ± 1	(0.8 ± 2.6) × 10^4	7.5
NBD-PR-II	540 ± 1	525 ± 1	(2.0 ± 0.4) × 10^4	8.3
NBD-PR-III	547 ± 1	528 ± 1	(1.5 ± 0.5) × 10^4	8.1
NBD-PR-IV	536 ± 1	528 ± 1	(3.0 ± 0.4) × 10^4	8.5
NBD-pre-PR-II	547 ± 1	547 ± 1	not bind	
NBD-aminoethanol	546 ± 1	546 ± 1	not bind	

around 540 nm (Table 3) and a low quantum yield in their fluorescence intensities, which indicate that the NBD moiety is in a hydrophilic environment (Rajarathnam et al., 1989). However, in the presence of PC vesicles a blue shift in the emission maximum and an increase in the fluorescence intensity of the NBD group were observed for the four PRs but not for pre-PR-II. The change in the spectrum of the NBD group reflects its relocation to a more hydrophobic environment, i.e., to the phospholipid vesicles (Chattopadhyay & London, 1987; Rajarathnam et al., 1989).

Binding Experiments and Determination of Partition Coefficients. The sensitivity of the NBD moiety to its environment facilitated its use in generating binding isotherms for NBD-labeled peptides, from which partition coefficients could be calculated as previously described (Rapaport & Shai, 1991). In the peptide binding experiments, a zwitterionic phospholipid (PC) was used to avoid the influence of phospholipid head group charges on the binding processes. The binding experiments were performed as described in Materials and Methods. The resultant increases in the fluorescence intensities of the NBD-labeled peptides were plotted as a function of lipid/peptide molar ratios to yield conventional binding curves (see Figure 2 for NBD-labeled PR-I as an example). Since the concentrations of the NBD-labeled peptides in the mixtures were low and the lipid/peptide molar ratios were very high, it was assumed that the peptides did not disrupt the bilayer structure. When unlabeled peptides were titrated with lipids, up to the maximal concentration used with NBD-labeled peptides, the fluorescence intensities of the solutions, after subtracting the contribution of the vesicles, remained unchanged.

The binding isotherms were then analyzed as described in Materials and Methods. Conventional binding isotherms were obtained by plotting X_b* (molar ratio of bound peptide per 60% of the total lipid assumed to be in the outer leaflet) versus C_f (the equilibrium concentration of free peptide in the solution) (see Figure 3, panels A, B, C, and D, for NBD-labeled PR-I, PR-II, PR-III, and PR-IV, respectively). The surface partition coefficients, K_p*, were estimated by extrapolating the initial slopes of the curves to zero C_f values. The estimated surface partition coefficients, K_p*, and the calculated free enthalpies of binding $\Delta G_{binding}$ (Reynolds et al., 1974), of the NBD-labeled peptides are listed in Table 3. The K_p* and $\Delta G_{binding}$ values obtained are within the range calculated for the P region of the *Shaker* K^+ channel (Peled & Shai, 1993) and for various membrane binding polypeptides, such as cytotoxins (Stankowski & Schwarz, 1990; Thiaudière et al., 1991; Rapaport & Shai, 1991; Gazit & Shai, 1993), signal peptides (Portlock et al., 1992), and antibacterial peptides (Pouny et al., 1992).

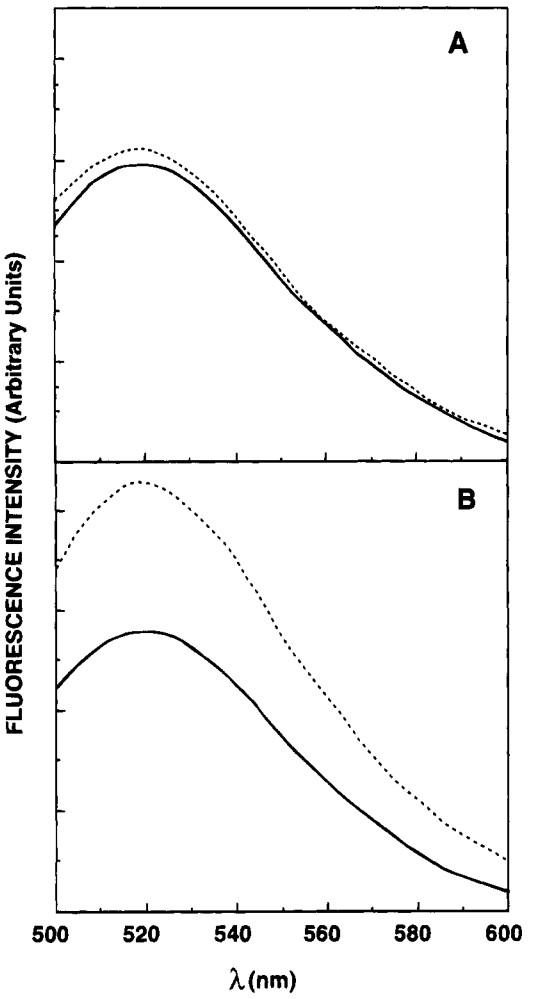

FIGURE 4: Changes in the fluorescence of NBD-PR-I upon addition of unlabeled peptides. The spectrum of NBD-PR-I (0.04 μM) was determined in the presence of PC vesicles (175 μM) in buffer, with (- - -) or without (—) 0.04 μM PR-III (A) and PR-II (B). The excitation wavelength was set at 470 nm, and emission was scanned from 500 to 600 nm.

Assembly of the PR Segments within Phospholipid Membranes. To evaluate whether the PR-derived peptides could form heteroaggregates within the membranes, two types of experiments were performed: (i) The changes in the fluorescence of the NBD group upon the interaction of a particular NBD-labeled segment with unlabeled segments were measured. Such changes are expected to occur only if the interaction between the segments causes a significant change in the environment of the NBD moiety, either by changing the orientation of the NBD-labeled peptide or by changing its aggregation state such that quenching or dequenching of the NBD fluorescence can occur. (ii) RET experiments between donor- and acceptor-labeled peptides were performed.

(i) Interaction of NBD-Labeled Peptides with Unlabeled Peptides. In a typical experiment NBD-labeled peptide (0.04 μM) was mixed with PC phospholipid LUV in buffer. The fluorescence of the solution was then measured with and without 0.04 μM of other unlabeled peptides. Figure 4 shows examples of the profiles obtained with NBD-PR-I/PR-III (panel A) and NBD-PR-I/PR-II (panel B) pairs. The addition of PR-III to NBD-PR-I did not significantly affect the fluorescence intensity of the NBD group. However, a marked increase in the fluorescence of NBD and a slight

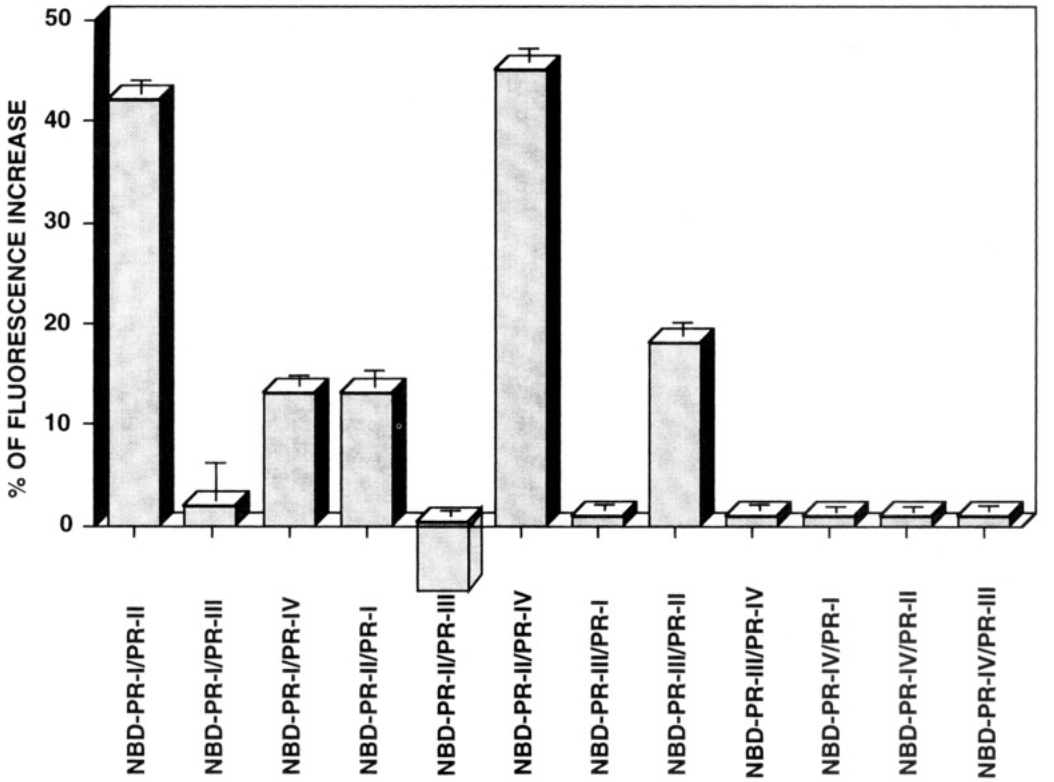

FIGURE 5: Percent of fluorescence increase of NBD-labeled PRs (final concentration, 0.04 μM) upon addition of unlabeled peptides (final concentration, 0.04 μM) using PC LUV (175 μM phospholipids) in buffer. The excitation wavelength was set at 470 nm. Emission spectra were recorded from 500 to 600 nm.

blue shift in the emission maximum occurred (three experiments) when PR-II was added to NBD-PR-I. In such a case, a change in fluorescence indicates that the two peptides interacted with each other, and as a result of this interaction the NBD moiety moved to a more hydrophobic environment, i.e., to the hydrophobic lipid core of the membrane. To determine whether the increases in the NBD fluorescence had some contributions from dequenching of the NBD fluorescence due to the dilution of the NBD-labeled monomers, similar experiments were performed with the environmentally insensitive Rho-labeled peptides. No changes were observed in the intensity of the emission spectra of Rho-peptides due to the addition of unlabeled peptides (data not shown). We may conclude, therefore, that dequenching of the NBD fluorescence due to the dilution of the NBD-labeled monomers is negligible. Figure 5 summarizes the results that were obtained with all other combinations. Significant changes occurred only with the pairs NBD-PR-I/PR-II, NBD-PR-I/PR-IV, NBD-PR-II/PR-I, NBD-PR-II/PR-III, NBD-PR-II/PR-IV, and NBD-PR-III/PR-II, suggesting that these pairs coassemble in their membrane-bound state.

It should be noted that, in those pairs where significant changes in the fluorescence of the NBD moiety did not occur, two explanations may be considered: (i) the particular pair is not coassembled, and (ii) the particular pair is coassembled, but the fluorescence of the NBD moiety is not affected, either because the NBD-labeled peptide does not change its position during the assembly proccess or because the site of the interaction is far from the NBD moiety. The latter is demonstrated with NBD-PR-IV in which the NBD moiety is attached to the N-terminal amino acid of the extended hydrophilic part of the peptide. The addition of the three unlabeled PRs did not affect its fluorescence. Therefore, to further evaluate the ability of the PRs to coassemble in their membrane-bound state, RET measurements were performed (Gazit & Shai, 1993) as will be described in the following section.

(ii) Resonance Energy Transfer Experiments. In these experiments only those PRs the NBD fluorescence of which was not affected by the addition of unlabeled counterpart segment were used as donors. Examples of profiles of the energy transfer that occurred with NBD-PR-III/Rho-PR-I and NBD-PR-IV/Rho-PR-II, in the presence of PC phospholipid vesicles, are depicted in panels A and B, respectively, of Figure 6. Rho-PR-I (final concentration, 0.04 μM) added to a solution containing NBD-PR-III (0.04 μM) preequilibrated with PC phospholipid LUV (175 μM) did not significantly affect the fluorescence of the donor (Figure 6A), in agreement with the observation that unlabeled PR-III did not affect significantly the NBD fluorescence of PR-I (Figure 5). However, when Rho-PR-II (final concentration, 0.04 μM) was added to a solution containing NBD-PR-IV (0.04 μM) preequilibrated with PC LUV (175 μM), the fluorescence of the donor was quenched significantly (Figure 6B). To determine the actual percentage of energy transfer, the amounts of lipid-bound acceptors (Rho-peptides) at the acceptor peptide concentration were calculated from the binding isotherms of the corresponding NBD-labeled peptides as previously described (Pouny et al., 1992). The experimentally derived percentages of energy transfer obtained for the various donor/acceptor pairs are depicted in Figure 7. We would expect approximately 3% RET if a random distribution of monomers occurred (Fung & Stryer, 1978), assuming an R_0 of 51 Å, which was previously calculated for the NBD/Rho donor/acceptor pair (Gazit & Shai, 1993). A high percentage of energy transfer was obtained with the pairs PR-I/PR-II, PR-I/PR-IV, PR-II/PR-

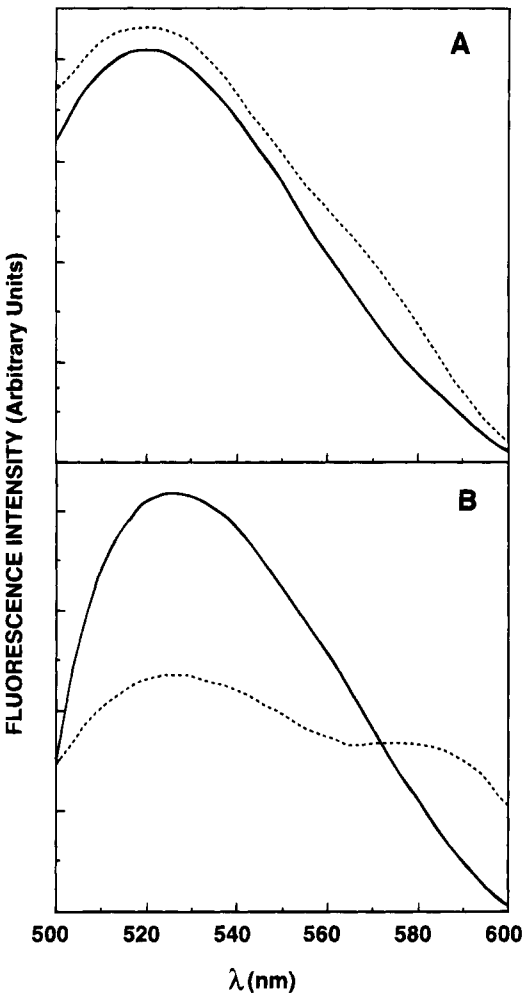

FIGURE 6: Fluorescence energy transfer resulting upon addition of Rho-peptide (acceptor) to NBD-peptide (donor). The spectrum of NBD-peptide (0.04 μM) was determined in the presence of PC LUV (175 μM phospholipids) in buffer, with (- - -) or without (—) 0.04 μM Rho-peptide. Panel A, NBD-PR-III/Rho-PR-I pair; panel B, NBD-PR-IV/Rho-PR-II pair. The excitation wavelength was set at 450 nm, and emission was scanned from 500 to 600 nm.

III, and PR-II/PR-IV, which confirms the results obtained in Figure 5. The RET experiments revealed that the PR-III/PR-IV pair also coassembles. Thus, from the data obtained with the NBD fluorescence studies (previous section) and the RET experiments we may conclude that, besides the PR-I/PR-III pair, all other pairs form heteroaggregates in their membrane-bound state. It should also be noted that none of the four PR segments coassemble with membrane-bound pardaxin, which contains approximately 50% α-helical structure (Shai et al., 1990; data not shown).

DISCUSSION

The pore-lining region of the K^+ channel is postulated to contain a tetramer of identical PRs, while the pore region of the Na^+ channels is postulated to contain four homologous PRs. The data reveal that although the PR segments of the Na^+ channel differ significantly in their primary sequences (Table 1) and also differ from the PR of the *Shaker* K^+ channel, they all bind with the same affinity to phospholipid membranes. These data are in line with the proposal that they have equivalent roles in participating in the formation of the hydrophobic core of the channel. It should be noted, however, that one amino acid substitution in the PR of the *Shaker* K^+ channel caused a 5-fold decrease in the partition coefficient of the resultant analog (Peled & Shai, 1993). Furthermore, slight changes in the amino acid composition of other biologically active membrane-interacting polypeptides significantly decreased or abolished their binding to membranes (Strahilevitz et al., 1994; Gazit et al., 1994).

An interesting observation is that, besides the PR-I/PR-III pair, all other combinations form heteroaggregates in their membrane-bound state (Figures 5 and 7). Furthermore, as a result of these interactions, the N-termini of PR-I and PR-II moved to more hydrophobic environments (Figure 5). The ability of the segments to form heteroaggregates in their membrane-bound state appears to be at least partially specific, since PR-I and PR-III do not coassemble (Figures 5 and 7), and neither of the segments coassembles with the α-helical pardaxin. These findings are in line with accumulating data showing the existence of interaction sites and recognition between transmembrane segments of membrane proteins. Some examples: glycophorin A (Bormann et al., 1989; Lemmon et al., 1992), bacteriorhodopsin (Kahn & Engelman, 1992), T cell receptor complex (Bonifacino et al., 1990a, 1990b; Manolios et al., 1990), tyrosine kinase receptor family (Sternberg & Gullick, 1990), aspartate sensory receptor of *Escherichia coli* (Lynch & Koshland, 1991), lactose permease of *Escherichia coli* (Sahin-Toth et al., 1992), helix-I and helix-II of *Bacillus thuringiensis* var. israelensis cytolytic toxin (Gazit & Shai, 1993), Isk channel protein (Ben-Efraim et al., 1994), and *Sendai* virus (Rapaport & Shai, 1994). These examples and others [see review by Lemmon and Engelman (1992)] suggest that transmembrane segments can contribute to specific recognition and assembly in other proteins as well.

These results therefore support the hypothesis that PR segments are packed in close proximity in the hydrophobic lumen of the Na^+ channel. These closely packed PRs may have a role as structural elements that participate in mediating the appropriate association of the hydrophobic core of Na^+ channel domains as previously proposed for K^+ channels (Li et al., 1992; McCormack et al., 1990; Pak et al., 1991; Peled & Shai, 1993; VanDongen et al., 1990). It is tempting to speculate that the fact that PR-I and PR-III are the only pair that do not coassemble in their membrane-bound state may indicate a preferential organization of these segments such that PR-I and PR-III are not adjacent.

It should be indicated that according to current Na^+ channel models, although the PRs are located within the membrane, they are surrounded by other transmembrane segments and therefore are not in direct contact with the membrane lipids. Our findings that the PR segments interact with membranes are relevant considering the following: (i) The ability of the PRs to interact strongly with a hydrophobic surface (i.e., phospholipid membranes, Table 3) may indicate their preferential location within the bundle of the hydrophobic α helices that form the pore. (ii) A "two-stage" model for membrane protein folding and oligomerization has been proposed (Popot et al., 1987; Popot & Engelman, 1990). In this two-stage model, the final structure in membranes results from the packing of smaller elements, each of which reaches thermodynamic equilibrium with the lipid and aqueous phases before packing. This model is supported by a number of studies with bacteriorhodopsin (Popot et al., 1990; Kahn & Engelman, 1992) and *E. coli* Lac permease (Sahin-Toth et al., 1992) showing that in vitro assembly of

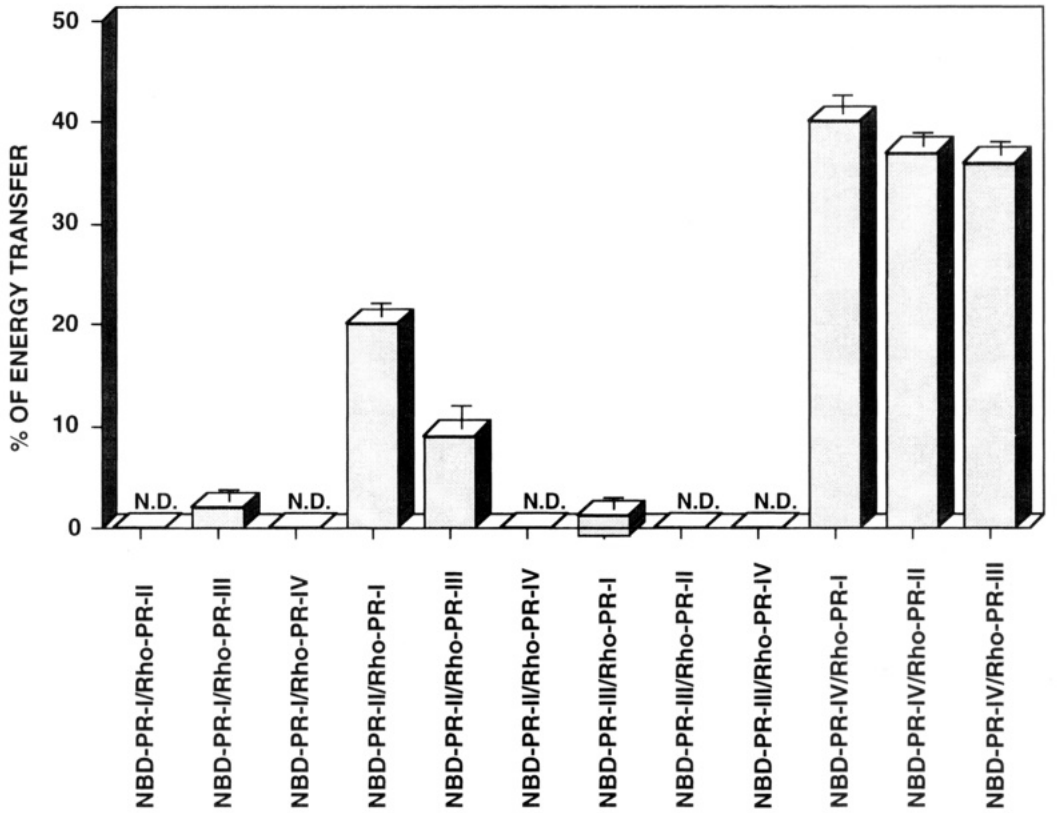

FIGURE 7: Percentage of fluorescence energy transfer resulting upon addition of Rho-peptides (final concentration, 0.04 μM) to NBD-peptides (final concentration, 0.04 μM) using PC LUV (175 μM phospholipids) in buffer. The percentage of energy transfer was calculated as described in Materials and Methods. A random distribution of the monomers (Fung & Stryer, 1978), assuming an R_0 of 51.1 Å as has been calculated for the NBD/Rho pair (Gazit & Shai, 1993), would give ~3% RET. N.D., not determined.

separated transmembrane segments into functional proteins may occur within a bilayer environment.

Various structural models have been proposed for pore regions of voltage-activated channels. These include α-helical, long β-barrel, short β-barrel, and mixed α-helical and β-barrel structures (Guy & Conti, 1990; Yellen et al., 1991; Hartmann et al., 1991; Yool & Schwarz, 1991; Durell & Guy, 1992; Kirsch et al., 1992; Lipkind & Fozzard, 1994). The CD spectroscopy indicated that the three segments (PR-I, PR-II, and PR-III) adopt ~30% α-helical structure in hydrophobic environments (40% TFE/water and 1% SDS) (Figure 1; Table 2). PR-IV contains the smallest fraction of α-helical structure, but is also the only extended form among the PRs synthesized. Unfortunately, its spectrum therefore cannot be compared with those of the other PRs. The finding that the segments adopt similar partial α-helical structures in two very different hydrophobic environments (Figure 1; Table 2), may indicate that the segments also contain partial α-helical structures in their native environment, i.e., the hydrophobic core of the channel. In support of this, recent studies have shown a correlation between the structure and the organization of synthetic peptides and those of their parent molecules. Such studies were performed for both soluble (Jaenicke, 1991; Dyson et al., 1992) and membrane proteins (Kahn et al., 1992; Lemmon & Engelman, 1992). Other examples come from studies showing that membrane-interacting polypeptides (Terwilliger & Eisenberg, 1982; Lovejoy et al., 1992) and various synthetic segments from bacteriorhodopsin (Barsukov et al., 1992) and from the pore region of δ-endotoxin (Gazit & Shai, 1993) adopt conformations similar to those of the relevant segments within the intact protein as determined by X-ray data. Further support for the partial helical structures of the PRs of the Na^+ channel comes from recent models proposed for the pore region of the channels (Guy & Durell, 1995).

ACKNOWLEDGMENT

We thank Dr. H. Robert Guy for his helpful comments.

REFERENCES

Armstrong, C. M. (1992) *Physiol. Rev. 72 (Suppl.)* 5−13.
Backx, P. H., Yue, D. T., Lawrence, J. H., Marban, E., & Tomaselli, G. F. (1992) *Science 257*, 248−251.
Barchi, R. L. (1988) *Annu. Rev. Neurosci. 11*, 455−495.
Barsukov, I. L., Nolde, D. E., Lomize, A. L., & Arseniev, A. S. (1992) *Eur. J. Biochem. 206*, 665−672.
Bartlett, G. R. (1959) *J. Biol. Chem. 234*, 466−468.
Ben-Efraim, I., Strahilevitz, J., Bach, D., & Shai, Y. (1994) *Biochemistry 33*, 6966−6973.
Beschiaschvili, G., & Seelig, J. (1990) *Biochemistry 29*, 52−58.
Bonifacino, J. S., Suzuki, C. K., & Klausner, R. D. (1990a) *Science 247*, 79−82.
Bonifacino, J. S., Cosson, P., & Klausner, R. D. (1990b) *Cell 63*, 503−513.
Bormann, B. J., Knowles, W. J., & Marchesi, V. T. (1989) *J. Biol. Chem. 264*, 4033−4037.
Catterall, W. A. (1992) *Physiol. Rev. 72 (Suppl.)* S15−S48.
Chattopadhyay, A., & London, E. (1987) *Biochemistry 26*, 39−45.
Chen, Y. H., Yang, J. T., & Chau, K. H. (1974) *Biochemistry 13*, 3350−3359.
Durell, S. R., & Guy, H. R. (1992) *Biophys. J. 62*, 238−250.
Dyson, H. J., Merutka, G., Waltho, J. P., Lerner, R. A., & Wright, P. E. (1992) *J. Mol. Biol. 226*, 795−817.
Frey, S., & Tamm, L. K. (1990) *Biochem. J. 272*, 713−719.
Fung, B. K.-K., & Stryer, L. (1978) *Biochemistry 17*, 5241−5248.
Gazit, E., & Shai, Y. (1993) *Biochemistry 32*, 12363−12371.

Gazit, E., Lee, W.-J., Brey, P. T., & Shai, Y. (1994) *Biochemistry 33*, 10681−10692.
Goulding, E. H., Tibbs, G. R., Liu, D., & Siegelbaum, S. A. (1993) *Nature 364*, 61−64.
Greenblatt, R. E., Blatt, Y., & Montal, M. (1985) *FEBS Lett. 193*, 125−134.
Greenfield, N., & Fasman, G. D. (1969) *Biochemistry 8*, 4108−4116.
Guy, H. R., & Seetharamulu, P. (1986) *Proc. Natl. Acad. Sci. U.S.A. 83*, 508−512.
Guy, H. R., & Conti, F. (1990) *Trends Neurosci. 13*, 201−206.
Guy, H. R., & Durell, S. R. (1995) Structural Models of Na^+, Ca^{2+}, and K^+ channels, in *Ion Channels and Genetic Diseases 48th Annual Symposium of Society of General Physiologist* (Dawson, D., Ed.) The Rockeffeler University Press (in press).
Hartmann, H. A., Kirsch, G. E., Drewe, J. A., Taglialatela, M., Joho, R. H., & Brown, A. M. (1991) *Science 251*, 942−944.
Heginbotham, L., & MacKinnon, R. (1992) *Neuron 8*, 483−491.
Heinemann, S. H., Terlau, H., Stühmer, W., Imoto, K., & Numa, S. (1992) *Nature 356*, 441−443.
Jaenicke, R. (1991) *Biochemistry 30*, 3147−3161.
Kahn, T. W., & Engelman, D. M. (1992) *Biochemistry 31*, 6144−6151.
Kenner, R., & Aboderin, A. (1971) *Biochemistry 10*, 4433−4440.
Kirsch, G. E., Drewe, J. A., Hartmann, H. A., Taglialatela, M., de Biasi, M., Brown, A. M., & Joho, R. H. (1992) *Neuron 8*, 499−505.
Kontis, K. J., & Goldin, A. L. (1993) *Mol. Pharmacol. 43*, 635−644.
Lemmon, M. A., & Engelman, D. M. (1992) *Curr. Opin. Struct. Biol. 2*, 511−518.
Lemmon, M. A., Flanagan, J. M., Hunt, J. F., Adair, B. D., Bormann, B. J., Dempsey, C. E., & Engelman, D. M. (1992) *J. Biol. Chem. 267*, 7683−7689.
Li, M., Jan, Y. N., & Jan, L. Y. (1992) *Science 257*, 1225−1230.
Lipkind, G. M., & Fozzard, H. A. (1994) *Biophys. J. 66*, 1−13.
Lovejoy, B., Akerfeldt, K. S., DeGrado, W. F., & Eisenberg, D. (1992) *Protein Sci. 1*, 1073−1077.
Lynch, B. A., & Koshland, D. E., Jr. (1991) *Proc. Natl. Acad. Sci. U.S.A. 88*, 10402−10406.
MacKinnon, R., & Miller, C. (1989) *Science 245*, 1382−1385.
MacKinnon, R., & Yellen, G. (1990) *Science 250*, 276−279.
MacKinnon, R., Heginbotham, L., & Abramson, T. (1990) *Neuron 5*, 767−771.
Manolios, N., Bonifacino, J. S., & Klausner, R. D. (1990) *Science 249*, 274−277.
Mao, D., & Wallace, B. A. (1984) *Biochemistry 23*, 2667−2673.
Mayer, L. D., Hope, M. J., & Cullis, P. R. (1986) *Biochim. Biophys. Acta 858*, 161−168.
McCormack, K., Lin, J. W., Iverson, L. E., & Rudy, B. (1990) *Biochem. Biophys. Res. Commun. 171*, 1361−1371.
Merrifield, R. B., Vizioli, L. D., & Boman, H. G. (1982) *Biochemistry 21*, 5020−5031.
Noda, M., Ikeda, T., Kayano, T., Suzuki, H., Takeshima, H., Kurasaki, M., Takahashi, H., & Numa, S. (1986a) *Nature 320*, 188−192.
Noda, M., Ikeda, T., Suzuki, T., Takeshima, H., Takahashi, H., Kuno, M., & Numa, S. (1986b) *Nature 322*, 826−828.
Pak, M. D., Baker, K., Covarrubias, M., Butler, A., Ratcliffe, A., & Salkoff, L. (1991) *Proc. Natl. Acad. Sci. U.S.A. 88*, 4386−4390.
Papahadjopoulos, D., & Miller, N. (1967) *Biochim. Biophys. Acta 135*, 624−638.
Peled, H., & Shai, Y. (1993) *Biochemistry 32*, 7879−7885.
Popot, J.-L., & Engelman, D. M. (1990) *Biochemistry 29*, 4031−4037.
Popot, J.-L., Gerchman, S.-E., & Engelman, D. M. (1987) *J. Mol. Biol. 198*, 655−676.
Portlock, S. H., Lee, Y., Tomich, J. M., & Tamm, L. K. (1992) *J. Biol. Chem. 267*, 11017−11022.
Pouny, Y., Rapaport, D., & Shai, Y. (1992) *Biochemistry 31*, 12416−12423.
Pusch, M., Noda, M., Stühmer, W., Numa, S., & Conti, F. (1991) *Eur. Biophys. J. 20*, 127−133.
Rajarathnam, K., Hochman, J., Schindler, M., & Ferguson-Miller, S. (1989) *Biochemistry 28*, 3168−3176.
Rapaport, D., & Shai, Y. (1991) *J. Biol. Chem. 266*, 23769−23775.
Rapaport, D., & Shai, Y. (1992) *J. Biol. Chem. 267*, 6502−6509.
Rapaport, D., & Shai, Y. (1994) *J. Biol. Chem. 269*, 15124−15131.
Reynolds, J. A., Gilbert, D. B., & Tanford, C. (1974) *Proc. Natl. Acad. Sci. U.S.A. 71*, 2925−2927.
Rizzo, V., Stankowski, S., & Schwarz, G. (1987) *Biochemistry 26*, 2751−2759.
Sahin-Toth, M., Dunten, R. L., Gonzalez, A., & Kaback, H. R. (1992) *Proc. Natl. Acad. Sci. U.S.A. 89*, 10547−10551.
Sato, C., & Matsumoto, G. (1992) *Biochem. Biophys. Res. Commun. 186*, 1158−1167.
Schwarz, G., Stankowski, S., & Rizzo, V. (1986) *Biochim. Biophys. Acta 861*, 141−151.
Schwarz, G., Gerke, H., Rizzo, V., & Stankowski, S. (1987) *Biophys. J. 52*, 685−692.
Shai, Y., Bach, D., & Yanovsky, A. (1990) *J. Biol. Chem. 265*, 20202−20209.
Stankowski, S., & Schwarz, G. (1990) *Biochim. Biophys. Acta 1025*, 164−172.
Sternberg, M. J. E., & Gullick, W. J. (1990) *Protein Eng. 3*, 245−248.
Strahilevitz, J., Mor A., Nicolas, P., & Shai, Y. (1994) *Biochemistry 33*, 10951−10960.
Tang, S., Mikala, G., Bashinski, A., Yatani, A., Varadi, G., & Schwartz, A. (1993) *J. Biol. Chem. 268*, 13026−13029.
Terlau, H., Heinemann, S. H., M., Stühmer, W., Pusch, M., Conti, F., Imoto, K., & Numa, S. (1991) *FEBS Lett. 293*, 93−96.
Terwilliger, T. C., & Eisenberg, D. (1982) *J. Biol. Chem. 257*, 6010−6015.
Thiaudière, E., Siffert, O., Talbot, J. C., Bolard, J., Alouf, J. E., & Dufourcq, J. (1991) *Eur. J. Biochem. 195*, 203−213.
VanDongen, A. M. J., Frech, G. C., Drewe, J. A., Joho, R. H., & Brown, A. M. (1990) *Neuron 5*, 433−443.
Yellen, G., Jurman, M. E., Abramson, T., & MacKinnon, R. (1991) *Science 251*, 939−942.
Yool, A. J., & Schwarz, T. L. (1991) *Nature 349*, 700−704.
Wu, C. S. C., Ikeda, K., & Yang, J. T. (1981) *Biochemistry 20*, 566−570.

BI950121P